Animal Nutrition 18 (2024) 107–118

Contents lists available at ScienceDirect

Animal Nutrition

journal homepage: http://www.keaipublishing.com/en/journals/aninu/

Original Research Article

Activation of skeletal carbohydrate-response element binding protein (ChREBP)-mediated de novo lipogenesis increases intramuscular fat content in chickens

Peng Wang, Haihan Xiao, Tian Wu, Qinghua Fu, Xudong Song, Yameng Zhao, Yan Li, Jieping Huang, Ziyi Song*

Guangxi Key Laboratory of Animal Breeding, Disease Control and Prevention, College of Animal Science and Technology, Guangxi University, Nanning, Guangxi 530004, China

ARTICLE INFO

Article history:
Received 19 August 2023
Received in revised form
10 April 2024
Accepted 10 April 2024
Available online 16 April 2024

Keywords:
Chicken
Meat quality
Intramuscular fat
Carbohydrate-response element binding protein
Fructose

ABSTRACT

The intracellular lipids in muscle cells of farm animals play a crucial role in determining the overall intramuscular fat (IMF) content, which has a positive impact on meat quality. However, the mechanisms underlying the deposition of lipids in muscle cells of farm animals are not yet fully understood. The purpose of this study was to determine the roles of carbohydrate-response element binding protein (ChREBP) and fructose in IMF deposition of chickens. For virus-mediated ChREBP overexpression in tibialis anterior (TA) muscle of chickens, seven 5-d-old male yellow-feather chickens were used. At 10 d after virus injection, the chickens were slaughtered to obtain TA muscles for analysis. For fructose administration trial, sixty 9-wk-old male yellow-feather chickens were randomly divided into 2 groups, with 6 replicates per group and 5 chickens per replicate. The chickens were fed either a basal diet or a basal diet supplemented with 10% fructose (purity $\geq$ 99%). At 4 wk later, the chickens were slaughtered, and breast and thigh muscles were collected for analysis. The results showed that the skeletal *ChREBP* mRNA levels were positively associated with IMF content in multiple species, including the chickens, pigs, and mice ($P < 0.05$). ChREBP overexpression increased lipid accumulation in both muscle cells in vitro and the TA muscles of mice and chickens in vivo ($P < 0.05$), by activation of the de novo lipogenesis (DNL) pathway. Moreover, activation of ChREBP by dietary fructose administration also resulted in increased IMF content in mice and notably chickens ($P < 0.05$). Furthermore, the lipidomics analysis revealed that ChREBP activation altered the lipid composition of chicken IMF and tented to improve the flavor profile of the meat. In conclusion, this study found that ChREBP plays a pivotal role in mediating the deposition of fat in chicken muscles in response to fructose-rich diets, which provides a novel strategy for improving meat quality in the livestock industry.

1. Introduction

As global living standards continue to improve, consumers are increasingly prioritizing the quality of meat over its quantity. However, decades of genetic selection for high growth rates and carcass yields have led to a decline in meat quality. Therefore, there is an urgent need to improve meat quality while maintaining high meat yields. Many factors can affect meat quality, including pH value, water-holding capacity, shear force, juiciness, flavor, and intramuscular fat (IMF) content (Rosenvold and Andersen, 2003). Of these factors, IMF is a critical element that positively affects meat quality (Frank et al., 2016).

* Corresponding author.
E-mail address: Ziyi.Song@gxu.edu.cn (Z. Song).

Peer review under responsibility of Chinese Association of Animal Science and Veterinary Medicine.

Production and Hosting by Elsevier on behalf of KeAi

https://doi.org/10.1016/j.aninu.2024.04.006

IMF refers to the fat deposited between fascial or muscle fiber bundles, mainly as adipocytes, but also within the cytoplasm of muscle cells (Hausman et al., 2014). Triglycerides (TG) are the main components of IMF, followed by phospholipids and cholesterol (Hocquette et al., 2010). While previous research on IMF deposition in farm animals has focused on the proliferation and differentiation of intramuscular adipocytes (Chen et al., 2017; Wang et al., 2020), there has been less attention paid to the lipids within muscle cells. Understanding how lipids accumulate in muscle cells is critical for developing new approaches to improving meat quality.

Currently, the most common type of diet used for monogastric animal production is corn–soybean meal, a carbohydrate-rich diet. Under this feeding condition, fat deposition is mainly determined by the balance between lipid biosynthesis and lipid breakdown. While the molecular events governing lipid synthesis in liver and adipose tissues have largely been revealed (Wallace and Metallo, 2020), the key molecules mediating lipid synthesis in muscles remain poorly defined.

Carbohydrate-response element binding protein (ChREBP), by forming heterodimers with its binding partner Max-like factor X (MLX), plays a critical role in linking carbohydrate metabolism to de novo lipogenesis (DNL) through the induction of transcription of glycolytic and lipogenic enzymes (Filhoulaud et al., 2013; Iizuka et al., 2004; Yamashita et al., 2001). ChREBP has two isoforms, ChREBP-α and ChREBP-β (Meng et al., 2016). While ChREBP-α is constitutively expressed in metabolically-active tissues such as liver, adipose tissues, and skeletal muscle, its transcriptional activity is highly controlled by intracellular carbohydrate levels (Iizuka et al., 2004). By contrast, ChREBP-β isoform is constitutively active in stimulating target gene expression, but its expression is very low and its transcription is induced in a feed-forward manner by ChREBP-α and itself (Bier et al., 2022). Although the physiological roles of ChREBP in liver (Yamashita et al., 2001), adipose tissue (Wang and Wollheim, 2002), intestine (Kato et al., 2018), kidney (Park et al., 2014), and pancreas have been reported (Chau et al., 2017), the function of ChREBP in skeletal muscle is still unexplored.

Based on the knowledge of ChREBP in other tissues or organs, it is hypothesized that ChREBP may play a role in carbohydrate-induced lipid biosynthesis in skeletal muscle. In the present study, it is found that the expression levels of skeletal ChREBP are positively correlated with IMF content in chickens, pigs, and mice. Overexpression of ChREBP-β in myoblasts activated the DNL pathway and promoted fat accumulation in vitro. This phenotype was recapitulated when ChREBP-β was overexpressed in tibialis anterior (TA) muscles of mice and chickens. Similarly, activation of ChREBP by 20% (wt/vol) fructose water administration increased IMF content in mice. Consistently, activation of ChREBP by dietary supplementation of 10% fructose increased IMF content and meat flavor of the chickens. Thus, our results indicate that activation of ChREBP-mediated DNL pathway by fructose provides a novel strategy to increase the IMF content in farm animals.

2. Materials and methods

2.1. Animal ethics statement

All animal studies were conducted in accordance with protocols approved by Guangxi University's Animal Ethics Committee (GXU2022-342).

2.2. Animals

For mice study, all male C57BL/6J mice were obtained from Changsha Tianqin Biotechnology Co. (Changsha, China) and housed under controlled environmental conditions with a 12/12 h light/dark cycle at 22 °C. For chicken study, commercial yellow-feather chickens (CYC) were purchased from Guangxi Fufeng Breeding Group (Nanning, China) and Lingshan local chickens (LLC) were obtained from a live-poultry market (Nanning, China). For pig study, Duroc pigs and Luchuan pigs were both purchased from the Animal Husbandry Research Institute of Guangxi. All the chickens and pigs were housed in an environmentally controlled room in Guangxi University Animal Experimental Center.

2.3. Adeno-associated virus (AAV) injection

For AAV-mediated gene overexpression in mice, the viruses (8.2×10^{10} genomic copies [GC] per TA muscle) were administered to the left TA muscles (AAV-Flag-green fluorescent protein [GFP]) or right TA muscles (AAV-Flag-ChREBP-β) of 15-wk-old male C57BL/6J mice via intramuscular injection. At 4 wk after AAV injection, the mice were euthanized and TA muscles were harvested for further analysis. For AAV-mediated gene overexpression in chickens, the viruses (9.3×10^{10} GC per TA muscle) were administered to the left TA muscles (AAV-Flag-GFP) or right TA muscles (AAV-Flag-ChREBP-β) of 5-d-old male CYC via intramuscular injection. At 10 d after AAV injection, the chickens were euthanized and TA muscles were harvested for further analysis. The viral vectors and viral stocks were prepared both by OBiO Technology (Shanghai, China).

2.4. Fructose administration

For fructose administration to mice, 6-wk-old mice were randomly assigned to receive either tap water or 20% fructose water. Caloric intake (kcal/d) was calculated using the following formula: Caloric intake (kcal/d) = [feed intake (g/d) × feed energy content (3.766 kcal/g)] + [drinking water intake (mL/d) × 20% fructose water energy content (0.8 kcal/mL)]. Twelve weeks later, the mice were euthanized after fasting for 4 h, and TA muscles were collected for further analysis. For fructose administration to chickens, sixty 9-wk-old male CYC were randomly divided into 2 groups, with 6 replicates per group and 5 chickens per replicate. The chickens were fed either a basal diet or a basal diet supplemented with 10% fructose (purity ≥ 99%). The basal ration was prepared according to the Feeding Standard of Chicken in China (NY/T 33-2004). The diet composition and nutrient levels are shown in Table 1. The basic nutrients in the diet were analyzed according to AOAC (2012) procedures as follows: crude protein (method 954.01), calcium using flame atomic absorption spectrometry (FAAS) technique (method 968.08), and phosphorus by colorimetric method (method 965.17). Lysine was determined by ion-exchange chromatography using an AA analyzer (Hitachi L-8800, Tokyo, Japan) after acid hydrolysis with 6 mol/L HCl and reflux at 110 °C for 24 h. Methionine and cystine were determined after oxidation with performic acid followed by hydrolysis with 6 mol/L HCl at 120 °C for 16 h and separation by reverse-phase HPLC (Agilent 1200, Santa Clara, CA). The metabolizable energy (ME) of the diet was calculated according to the equation of Kirchgessner and Roth (1983). At 4 wk later, the chickens were slaughtered after fasting for 12 h and breast and thigh muscles were collected for further studies.

2.5. Cell culture

The mouse C2C12 myoblasts were cultured at 37 °C (in 5% CO_2) in high glucose Dulbecco's modified Eagle's medium (DMEM; Gibco, United States) supplemented with 10% (vol/vol) fetal bovine serum (FBS) and 100 μg/mL penicillin–streptomycin solution (P1400, Beijing Solarbio Science & Technology Co., Ltd., China). Adipogenic induction was induced by shifting the completely

Table 1
Composition and nutrient levels of the basal diet (air-dry basis, %).

Item	Content
Ingredients	
Corn	58.00
Soybean meal	27.50
Wheat bran	8.20
Limestone	1.10
$CaHPO_4$	0.80
$NaHCO_3$	0.08
NaCl	0.20
Lard oil	2.20
Choline chloride (60%)	0.06
L-Lysine sulfate (70%)	0.50
DL-Methionine	0.18
L-Threonine	0.06
Phytase	0.02
Propionic acid	0.05
Sodium butyrate	0.05
Premix[1]	1.00
Total	100.00
Nutrient levels[2]	
ME, kcal/kg	2880
Crude protein	18.45
Ca	0.71
Total P	0.53
Digestible P	0.27
Lysine	1.23
Methionine	0.46
Cystine	0.35

ME = metabolizable energy.
[1] The premix provided the following per kilogram of diets: vitamin A, 6000 IU; vitamin D_3, 200 IU; vitamin E, 10 IU; vitamin K, 0.50 mg; vitamin B_{12}, 0.007 μg; pantothenic acid, 2.99 mg; riboflavin, 1.63 mg; Cu, 1.25 mg; Mn, 24.06 mg; Zn, 12.70 mg; Se, 0.06 mg; iodide, 0.35 mg.
[2] ME is a calculated value and the others are measured values.

confluent cells to DMEM containing 0.5 μmol/L IBMX (I7018, Sigma, United States), 1 μmol/L dexamethasone (D8040, Beijing Solarbio Science & Technology Co., Ltd., China), and 10 μg/mL insulin (I8830, Beijing Solarbio Science & Technology Co., Ltd., China) for 2 d. The cells were then maintained in DMEM containing 10 μg/mL insulin, with medium replaced every other day. Full differentiation was achieved in approximately 8 d.

2.6. Retroviral transduction

To obtain stable ChREBP-β-overexpressing C2C12 myoblasts, retroviral vectors were packaged and transduced as previously described (Song et al., 2022). Briefly, pMSCV-PIG-ChREBP-β (or pMSCV-PIG) and packaging plasmids (pUMVC and pCMV-VSV-G) were co-transfected into sub-confluent HEK293T cells using Lipofectamine 2000 Transfection Reagent (Invitrogen, United States) according to the manufacturer's instructions. Viral stocks were collected at 48 h and 72 h post-transfection, filtered through a 0.45-μm filter, and frozen at −80 °C. C2C12 myoblasts (20% to 30% confluent) were then infected with the retrovirus stocks containing 8 mg/mL polybrene. After 48 h, the cells were selected with 2 μg/mL puromycin (60210ES25, Yeasen, China).

2.7. Oil red O staining

Cellular Oil red O staining was performed according to previously described methods (Song et al., 2017). Briefly, the cells were washed once with 1× PBS and fixed with 4% paraformaldehyde for 30 min. Subsequently, the cells were washed again and stained with freshly prepared 60% Oil red O working solution for 30 min. After staining, the cells were washed 4 times with 1× PBS, and images were captured using a digital camera (Nikon p520) and an inverted microscope (Nikon ECLIPSE TS2). Tissue Oil red O staining was performed according to a previously described method (Wang et al., 2022). Muscle tissue was dissected and fixed in tissue fixative at 4 °C for frozen sectioning, followed by Oil red O staining. Sample sectioning and staining were performed at Wuhan Saiwei Biotechnology Co., Ltd. (Wuhan, Hubei Province, China). Images were collected using a light microscope (Biological Microscope ML31, MSHOT, Guangzhou, China).

2.8. Hematoxylin and eosin (H&E) staining

H&E staining was performed according to previously described methods (Wang et al., 2022). Muscle tissues were dissected and fixed in tissue-fixing liquid at 4 °C. The samples were subsequently sent to Xi'an Yike Biotechnology Service Co., Ltd. (Xi'an, China) for embedding, sectioning and H&E staining. Images were collected using a light microscope (Biological microscope ML31, MSHOT, Guangzhou, China), and the areas of muscle fibers were analyzed using Image J software (version 1.53t).

2.9. RNA extraction and quantitative real-time PCR (qRT-PCR)

RNA extraction and qRT-PCR were performed as previously described (Wang et al., 2022). Briefly, total RNA was extracted from cell or tissue samples using Trizol reagent (Life Technologies, United States) following the manufacturer's instructions. The quantity and quality of total RNA were determined using a spectrophotometer (Nanodrop 2000, Thermo Fisher, United States). Total cDNA was synthesized from 1 μg of total RNA using the RevertAid First Strand cDNA Synthesis Kit (Thermo Fisher, United States). Real-time PCR was performed on a LightCycler 480 II real-time PCR machine (Roche) using 2× RealStar Green Fast Mixture (A301-01, GenStar, Beijing, China), and specific primers for each gene were designed with the Primer designing tool from NCBI and are listed in Table 2. TATA-box binding protein (*Tbp*) was used as the invariant control.

2.10. Western blotting

Western blotting was performed according to previously described methods with some modifications (Fu et al., 2022). Briefly, cells or tissue powders were lysed using RIPA lysis buffer (IN-WB001, Invent, Plymouth, USA) with 1 mmol/L PMSF (P0100, Solarbio Technology Co., Beijing, China). The lysates were diluted with sample loading buffer (P0015L, Beyotime, Shanghai, China), boiled, and loaded onto a 10% SDS-PAGE gel. After electrophoresis, the proteins were transferred to a PVDF membrane, and the membranes were routinely washed and blocked with 5% non-fat dry milk in TBST. Then, the following antibodies and dilutions were used: anti-myosin heavy chain (MyHC) (MAB4470-SP, 1:3000) from R&D systems; anti-ChREBP (NBP2-44307, 1:500) from NOVUS; anti-peroxisome proliferator activated receptor gamma (PPARγ) (#2435, 1:1000) and anti-fatty acid synthase (FAS) (#3180, 1:500) from Cell Signaling Technology; anti-alpha-tubulin (AF5012, 1:3000) from Beyotime; anti-FLAG (M20008, 1:5000) from Abmart; anti-β-actin (HC201, 1:2000) from TransGen Biotech; anti-rabbit IgG (111-035-003, 1:3000) and anti-mouse IgG (115-035-003, 1:2000) from Jackson ImmunoResearch Laboratories (West Grove, PA, USA). Detection was

Table 2
The sequence of qPCR primers.

Gene	Species	Forward primer (5′–3′)	Reverse primer (5′–3′)
Acaca	Mouse	CCGAGAAAGCAGGGGATCTG	TACCCGACGCATGGTTTTCA
Acly	Mouse	GCTGTGCAGGGCATGCTGGA	CCATGGCAGCCACTGAGGGC
Adipoq	Mouse	GCCGCTTATGTGTATCGCTCAG	TTGCCAGTGCTGCCGTCATA
Cebpa	Mouse	TGGACAAGAACAGCAACGAG	TCACTGGTCAACTCCAGCAC
ChREBP	Mouse	GCTCAACGCTGCCATCAACTTG	GGTCGGATGAGGATGCTGAACA
Elovl6	Mouse	TCAACGAGAACGAAGCCATCCA	TTCATCAGATGCCGACCACCAA
Fabp4	Mouse	AAGAAGTGGGAGTGGGCTTTG	CTCTTCACCTTCCTGTCGTCTG
Fasn	Mouse	CACTGCATTGACGGCCGGGT	GGACAAGCCCAGGCTGCGAG
Glut4	Mouse	GTCCTCCTGCTTGGCTTCTTCA	ACTGGGTTTCACCTCCTGCTCT
MyhC	Mouse	GAAGTTGCATCCCTAAAGGCAG	AAGGCTTGTTCTGAGCCTCG
MyoD1	Mouse	GGCTCTCTCTGCTCCTTTGA	GTAGGGAAGTGTGCGTGCTC
MyoG	Mouse	AGGAAGTCTGTGTCGGTGGA	AGGCGCTCAATGTACTGGAT
Pparg	Mouse	CCAAGAATACCAAAGTGCGATCA	CCCACAGACTCGGCACTCAAT
Srebp1c	Mouse	AGGAGGACATCTTGCTGCTTCT	GATCTCTGCCAGTGTTGCCATG
Tbp	Mouse	ACTTCGTGCAAGAAATGCTGA	CAGTTGTCCGTGGCTCTCTT
Chrebp	Chicken	ATTGACCCGACCCTGACG	CATACTGGATGTACCACGCTCT
Thrsp	Chicken	ATCAAGCCCGTGGTGGAGC	CTTTGGTGTTTTTGGTGAGGTCG
β-Actin	Chicken	TGCGTGACATCAAGGAGAAG	TGCCAGGGTACATTGTGGTA
Acaca	Chicken	AACCTGCTAAACCCCTGG	AGTCCCAAATCCGAAAGG
Acss1	Chicken	TGGGAGATGTTACCACAC	GCAGAATACACCAAGAGAG
Acc1	Chicken	AATGGCAGCTTTGGAGGTGT	AATGGCAGCTTTGGAGGTGT
Scd1	Chicken	TTGTCTGATGGAGATCATGGCTTC	TGCTTGCCTTCAGGATTAAAGTGAG
Chrebp	Pig	CGACACACTCTTCACCACGA	TGAAGGTGTAGGCGTCTGTG
Tbp	Pig	GAACTGGCGGAAGTGACGTT	GCACAGCAAGAAAGAGTGATGC

Acaca = acetyl-CoA carboxylase alpha; *Acly* = ATP citrate lyase; *Adipoq* = adiponectin; *Cebpa* = CCAAT enhancer binding protein alpha; *ChREBP* = carbohydrate-response element binding protein; *Elovl6* = ELOVL fatty acid elongase 6; *Fabp4* = fatty acid binding protein 4; *Fasn* = fatty acid synthase; *Glut4* = glucose transporter 4; *MyhC* = myosin heavy chain; *MyoD1* = myogenic differentiation 1; *MyoG* = myogenin; *Pparg* = peroxisome proliferator activated receptor gamma; *Srebp1c* = sterol regulatory element binding transcription factor 1; *Tbp* = TATA-box binding protein; *Thrsp* = thyroid hormone responsive; *Acss1* = acyl-CoA synthetase short chain family member 1; *Acc1* = acetyl-CoA-carboxylase 1; *Scd1* = stearoyl-coenzyme A desaturase 1.

performed using chemiluminescence (Abbkine, Waltham, MA, USA) and the Bio-Rad Imaging System (Bio-Rad, CA, USA).

2.11. Measurement of TG and crude fat (CF)

Triglycerides in C2C12 cells as well as muscles of mice and chickens were measured using the TG Test Kit (A110-1-1, Nanjing Jiancheng Bioengineering Institute, China), following the manufacturer's instructions. Protein concentration in the samples was measured using the BCA Protein Quantitative Analysis Kit (Beyotime Biotechnology, Shanghai, China). The amount of TG was expressed as μmol/g protein. The CF content in the breast and thigh muscles of CYC was determined by the Soxhlet extraction method, using petroleum ether as a solvent, and expressed as a percentage of the fresh muscle tissue weight (Demirel et al., 2006).

2.12. Lipid extraction and lipidomic assay

The breast muscle samples from the chickens were homogenized with a 2:1 (vol/vol) mixture of chloroform and methanol, using a high-flux tissue grinder at 4 °C, and then centrifuged at 8000 × *g* for 20 min at 4 °C (Li et al., 2020). The organic layer was collected and dried using nitrogen gas. The lipids were then analyzed by Suzhou PANOMIX Biomedical Technology Co., Ltd. (Suzhou, China) using liquid chromatography-mass spectrometry (LC–MS). The data analysis process involved the following steps: first, the raw data were annotated according to the LIPID MAPS Structural Database (LMSD; http://www.lipidmaps.org/). Next, the data were evaluated separately using the orthogonal partial least squares discriminant analysis (OPLSDA) method, using the R package ropls. Lipids with a variable importance in projection (VIP) value > 1 in the partial least squares discriminant analysis (PLS–DA) and *P*-values <0.05 in the *t*-tests in both positive and negative ion modes were considered statistically significant and selected for further analysis.

2.13. RNA sequencing (RNA-seq)

RNA-seq analysis was conducted as previously described (Wang et al., 2022). Briefly, purified total RNA samples from ChREBP-β overexpressed C2C12 myoblasts and control samples were sent to Guangzhou Gene Denovo Biotech Co. Ltd. (Guangzhou, China) for library construction and sequencing. The raw RNA-seq data were deposited in the Gene Expression Omnibus data repository with the login number GSE228899. The data analysis process was as follows. First, all sequencing reads were mapped to the mm10 mouse genome using Bowtie2 and Tophat2. Next, the mapped reads were normalized as reads per kilobase of transcript per million mapped reads (RPKM). Differentially expressed genes (DEG) were identified using the RNA-seq processing tool DESeq2, with selection based on an adjusted *P*-value <0.05 and fold change (FC) > 1.5 or < 0.5. The DEG were visualized using R tools ggplot2 and heatmap. Gene set enrichment analysis (GSEA) was performed by ranking the normalized gene expression data according to the log2 FC, and then visualized using R package Cluster Profiler.

2.14. Statistical analysis

Data was assessed using unpaired Student's *t*-test (for two groups) or one-way analysis of variance (ANOVA; for multiple groups), with a probability of $P < 0.05$ considered statistically significant difference. Association of *ChREBP* gene expression with intracellular TG levels was examined by linear regression analysis. Results are presented as means and SEM. Statistical analysis and Figure preparation were performed using GraphPad Prism 8.0.

3. Results

3.1. IMF content is positively correlated with skeletal ChREBP levels

To investigate the role of ChREBP in IMF deposition, the relationship between *ChREBP* expression level and IMF content were

examined. The results are shown in Tables 3 and 4. The IMF content in the thigh muscle of CYC was significantly higher than that of the age- and diet-matched LLC, and the *ChREBP* mRNA level of the former was correspondingly higher ($P < 0.05$). Furthermore, a positive and significant correlation was found between the levels of IMF content and *ChREBP* expression in the thigh muscles of those chickens ($P = 0.044$), which was similarly observed in the longissimus dorsi of Duroc and Luchuan pigs ($P = 0.047$). Also, the relationship between *ChREBP* expression and IMF content in different-aged C57BL/6J mice was investigated and found that aged mice exhibited higher levels of both IMF content and ChREBP expression compared to young mice ($P < 0.001$), with a positive and significant correlation between IMF content and *ChREBP* expression ($P = 0.007$). Overall, these findings suggest that skeletal ChREBP may positively regulate IMF deposition in animals.

3.2. ChREBP overexpression promotes lipid accumulation in muscle cells

Next, to investigate the potential causal relationship between ChREBP levels and IMF content, C2C12 myoblasts were used as an in vitro model. Through retro-virus infection, ChREBP-β was successfully overexpressed in these cells (Fig. 1A to C). Under adipogenic condition, the control group maintained a classical myogenic phenotype with minimal lipid accumulation, while the ChREBP-β overexpression group exhibited a significant increase in lipid accumulation, as demonstrated by Oil red O staining (Fig. 1D). This result was further confirmed by TG measurements, which revealed a 2.5-fold increase in intracellular lipid content in the ChREBP-β overexpression group compared to the control (Fig. 1E). Consistent with these findings, the expression of lipogenic and adipogenic marker genes was notably induced by ChREBP-β overexpression ($P < 0.05$; Fig. 1F and G), while the expression of myogenic marker genes such as myogenic differentiation 1 (*MyoD1*), myogenin (*MyoG*), and *MyhC* was significantly inhibited ($P < 0.05$; Fig. 1H). These results were further validated by Western blotting (Fig. 1I). Taken together, these data suggest that increasing ChREBP expression in muscle cells can promote intracellular lipid accumulation.

3.3. Overexpression of ChREBP activates lipogenic pathway but inhibits myogenic pathway in muscle cells

To further elucidate how ChREBP promotes lipid accumulation in muscle cells in vitro, RNA-seq analyses were performed to assess the genome-wide effects of ChREBP overexpression on myoblasts transcription. The differential expression data showed that 447 genes were upregulated, while 946 genes were downregulated, in myoblasts with ChREBP overexpression compared to the control group (Fig. 2A). Cluster heatmap analyses of the DEG revealed that the upregulated and downregulated genes belonged to distinct pathways (Fig. 2B). Moreover, GSEA indicated that several upregulated gene sets were involved in the regulation of lipid biosynthetic processes, while many downregulated genes were associated with muscle cell development (Fig. 2C to E). Notably, the key lipogenic genes such as acetyl-CoA carboxylase alpha (*Acaca*), ATP citrate lyase (*Acly*), and *Fasn* were significantly upregulated in the lipid biosynthesis pathway (Fig. 2F), while pivotal myogenic genes such as *MyoD1* and *MyoG* were significantly downregulated in muscle cell development (Fig. 2G). These DEG were further confirmed using qRT-PCR ($P < 0.05$; Fig. 2H and I). Overall, these findings demonstrate that ChREBP-β overexpression alone is sufficient to activate the DNL pathway in myoblasts, which accounts for the substantial lipid accumulation in these cells under adipogenic conditions.

Table 4
The correlation coefficient between *ChREBP* expression and IMF content.

Gene	IMF content					
	Chicken[1]		Pig[2]		Mouse[3]	
	R^2	*P*-value	R^2	*P*-value	R^2	*P*-value
ChREBP	0.346	0.044*	0.665	0.047*	0.533	0.007*

IMF = intramuscular fat; *ChREBP* = carbohydrate-response element binding protein.
Values with an asterisk represent statistically significant differences (*$P < 0.05$).
[1] Data represent the mean value of 7 replicates each treatment ($n = 7$).
[2] Data represent the mean value of 3 replicates each treatment ($n = 3$).
[3] Data represent the mean value of 6 replicates each treatment ($n = 6$).

3.4. Skeletal overexpression of ChREBP increases IMF content in mice and in chickens

Next, to investigate whether overexpression of ChREBP in vivo also leads to an increase in IMF content, AAV injection was utilized to overexpress flag-tagged ChREBP-β in the right TA muscles of C57BL/6J mice, while flag-tagged GFP in AAV was injected in the left TA muscles of the mice as an internal control. After 4 wk, TA muscles were collected for analysis. The procedure was illustrated in Fig. 3A. The significant higher mRNA and protein levels of ChREBP demonstrated successful overexpression of ChREBP-β in TA muscles (Fig. 3B and C). Consistent with the in vitro data, ChREBP-β overexpression was able to activate the expression of lipogenic and adipogenic genes in TA muscles (Fig. 3D and E). Correspondingly, the intracellular TG content in TA muscles was almost doubled (Fig. 3F). However, ChREBP overexpression did not impact the total TA weight of the mice (Fig. 3G), possibly due to the reduction in muscle fiber diameter ($P < 0.001$; Fig. 3H and I).

Table 3
TG content and *ChREBP* expression level in muscle of different animals.

Item	Chicken[1]				Pig[2]				Mouse[3]			
	LLC	CYC	SEM	*P*-value	Duroc	Luchuan	SEM	*P*-value	1-mo-old mice	8-mo-old mice	SEM	*P*-value
TG, μmol/g protein	75.85	146.50*	31.120	0.042	183.60	240.90**	7.186	0.001	26.17	42.77**	3.616	0.001
Relative *ChREBP* expression	1.00	2.27*	0.250	0.027	1.00	1.28*	0.090	0.035	1.00	1.27***	0.037	<0.001

SEM = the standard error of the mean; LLC= Lingshan local chicken; CYC= commercial yellow-feather chicken; TG = triglyceride; *ChREBP* = carbohydrate-response element binding protein.
Values with asterisk represent statistically significant differences (*$P < 0.05$, **$P < 0.01$, ***$P < 0.001$).
[1] Data represent the mean value of 7 replicates each treatment ($n = 7$).
[2] Data represent the mean value of 3 replicates each treatment ($n = 3$).
[3] Data represent the mean value of 6 replicates each treatment ($n = 6$).

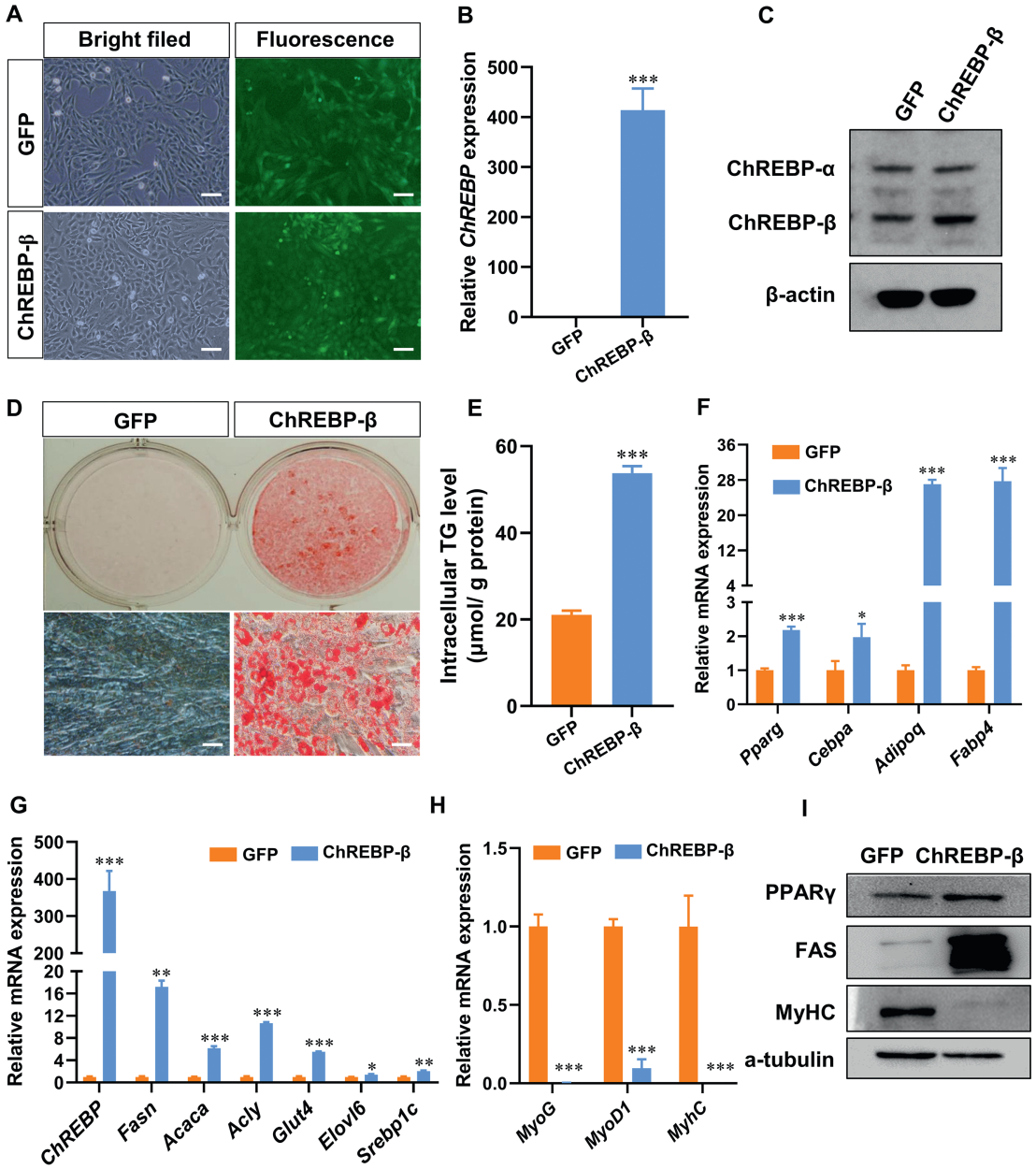

Fig. 1. ChREBP-β overexpression in muscle cells promotes lipid accumulation. (A) The retroviral-infected C2C12 myoblasts. Scale bar, 100 μm. (B to C) The analysis of ChREBP expression levels in C2C12 myoblasts by qRT-PCR and Western blotting. (D) Oil red O staining of C2C12 myoblasts overexpressing GFP or ChREBP-β under adipogenic induction for 7 d. Scale bar, 100 μm. (E) TG content in C2C12 myoblasts overexpressing GFP or ChREBP-β for 7 d of adipogenic induction. (F to H) qRT-PCR analysis of mRNA levels of (F) adipogenic genes, (G) lipogenic genes, and (H) myogenic genes. (I) Western blotting analysis for the expression of PPARγ, FAS, and MyHC proteins. GFP = green fluorescent protein; ChREBP-α = carbohydrate-response element binding protein-α; ChREBP-β = carbohydrate-response element binding protein-β; TG = triglyceride; *Pparg*/PPARγ = peroxisome proliferator activated receptor gamma; *Cebpa* = CCAAT enhancer binding protein alpha; *Adipoq* = adiponectin; *Fabp4* = fatty acid binding protein 4; *ChREBP* = carbohydrate-response element binding protein; *Fasn*/FAS = fatty acid synthase; *Acaca* = acetyl-CoA carboxylase alpha; *Acly* = ATP citrate lyase; *Glut4* = glucose transporter 4; *Elovl6* = ELOVL fatty acid elongase 6; *Srebp1c* = sterol regulatory element binding transcription factor 1; *MyoG* = myogenin; *MyoD1* = myogenic differentiation 1; *MyhC* = myosin heavy chain; a-tubulin = alpha-tubulin; All the results are shown as the means ± SEM; $^{*}P < 0.05$, $^{**}P < 0.01$, $^{***}P < 0.001$.

Subsequently, AAV-ChREBP-β was injected in the TA muscle of the 5-d-old chickens using a similar protocol to test whether ChREBP overexpression induces IMF accumulation in chickens. The viruses-injected muscles were harvested for analysis at 10 d later. First, the expression of ChREBP and its lipogenic target genes were examined by qRT-PCR. As shown in Tables 5 and 6, compared with the GFP-injected muscles, ChREBP-β-injected muscles had significantly higher expression of *ChREBP*, thyroid hormone responsive (*Thrsp*), *Acaca*, acyl-CoA synthetase short chain family member 1 (*Acss1*), acetyl-CoA-carboxylase 1 (*Acc1*) ($P < 0.05$), indicating ectopic overexpression of ChREBP-β activates lipogenesis in muscles of chickens. Consistent with the lipogenic genes expression, IMF content was also significantly elevated in ChREBP-overexpressed muscles ($P = 0.001$). Taken together, these results indicate that increasing skeletal ChREBP levels is sufficient to induce IMF deposition in both mice and chickens.

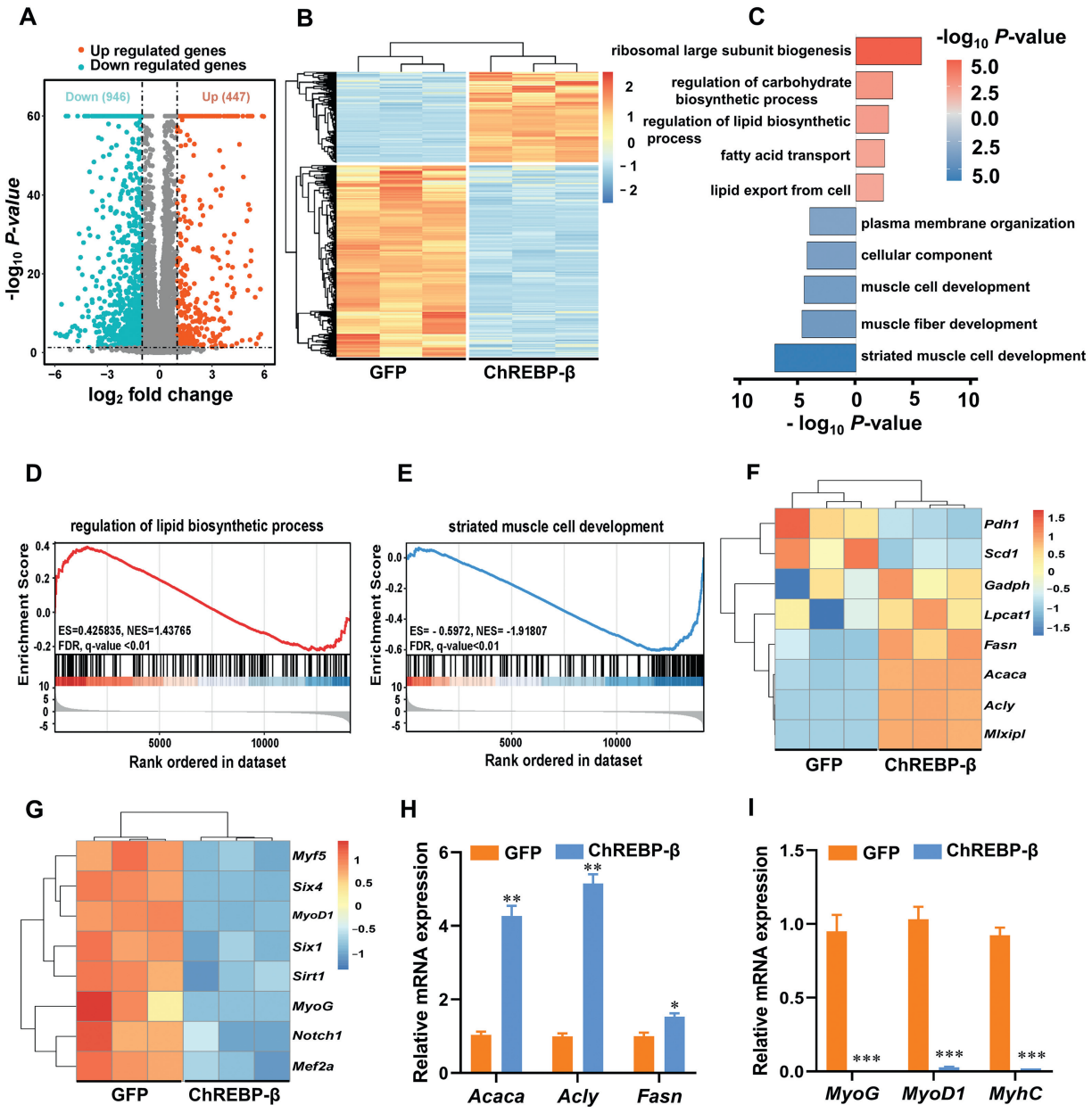

Fig. 2. RNA sequencing (RNA-seq) analysis reveals ChREBP-β overexpression in C2C12 myoblasts activates lipogenic pathway but inhibits myogenic pathway. (A) Volcano plot comparison of gene expression. (B) Cluster analysis of all differential genes. (C) Gene set enrichment analysis (GSEA) of differentially expressed genes. (D and E) GSEA analysis of the significantly upregulated (regulation of lipid biosynthetic process) and downregulated (muscle cell development) pathways. (F and G) Heat map of genes related with lipid synthesis and muscle development. (H and I) qRT-PCR analysis of lipogenic genes and myogenic genes. GFP = green fluorescent protein; ChREBP-β = carbohydrate-response element binding protein-β; ES = enrichment score; NES = normalized enrichment scores; FDR = false discovery rate; *Pdh1* = pyruvate dehydrogenase 1; *Scd1* = stearoyl-coenzyme A desaturase 1; *Gadph* = glyceraldehyde-3-phosphate dehydrogenase; *Lpcat1* = lysophosphatidylcholine acyltransferase 1; *Fasn* = fatty acid synthase; *Acaca* = acetyl-CoA carboxylase alpha; *Acly* = ATP citrate lyase; *Mlxipl* = MLX interacting protein-like; *Myf5* = myogenic factor 5; *Six4* = SIX homeobox 4; *MyoD1* = myogenic differentiation 1; *Six1* = SIX homeobox 1; *Sirt1* = sirtuin 1; *MyoG* = myogenin; *Notch1* = notch receptor 1; *Mef2a* = myocyte enhancer factor 2A; *MyhC* = myosin heavy chain. All data were collected from C2C12 cells overexpressing GFP or ChREBP-β without induction ($n = 3$). All the results are shown as the means ± SEM; *$P < 0.05$, **$P < 0.01$, ***$P < 0.001$.

3.5. Activation of ChREBP by fructose administration increases IMF content in mice

As it is difficult to perform transgenic overexpression of ChREBP in animal production, next, studies were conducted to investigate whether activation of ChREBP by dietary supplementation of fructose could elevate IMF content in vivo. To achieve this, mice were administered with 20% (wt/vol) fructose water for 12 wk. As shown in Tables 7 and 8, compared to the controls, mice with fructose administration almost doubled their drinking water consumption ($P < 0.001$). However, the mice reduced their feed intake by more than 50% to compensate for the calories obtained from fructose ($P < 0.001$). Overall, the total energy intake of the mice was not altered by fructose administration. Consistently, the bodyweight of the fructose-drinking mice showed a similar growth trend to the control mice. Furthermore, the weights of the gastrocnemius (GA) and TA muscles were not affected by fructose supplementation. Nevertheless, it was found that fructose administration substantially activated *ChREBP* and its downstream lipogenic genes expression in TA muscles ($P < 0.05$; Table 8). In

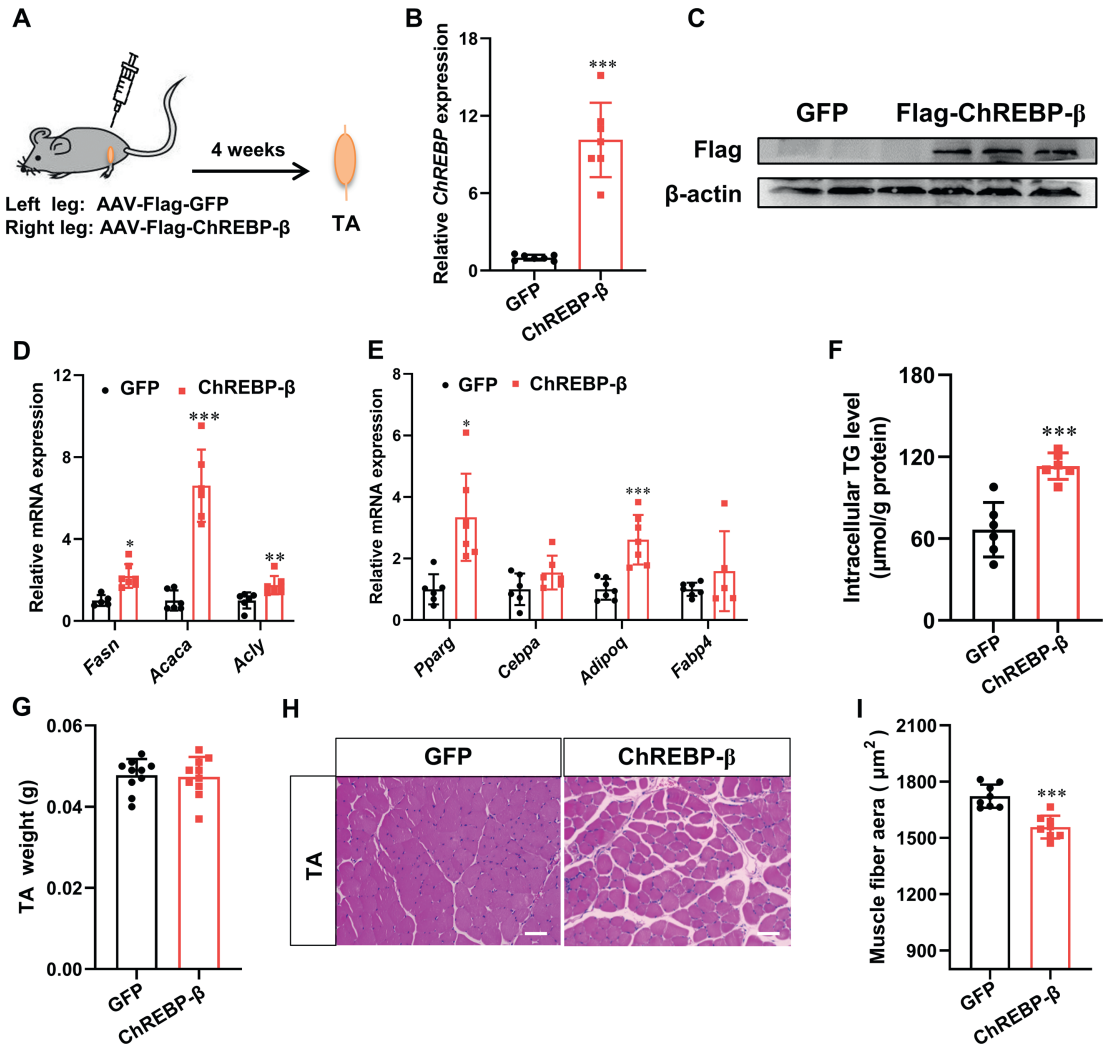

Fig. 3. AAV-mediated overexpression of ChREBP-β in mice TA muscles facilitates DNL pathway and increases TG accumulation. (A) Diagram of experimental design. (B) qRT-PCR analysis of ChREBP expression in TA muscles (n = 6 to 7). (C) Western blotting analysis of Flag-ChREBP-β expression in TA muscles (n = 3). (D and E) Relative mRNA levels of lipogenic genes and pan-adipocyte genes in TA muscles (n = 6 to 7). (F) TG content in TA muscles (n = 6). (G) The weight of TA muscles (n = 10). (H) Hematoxylin and eosin (H&E) staining of paraffin sections of TA muscles. Scale bar, 100 μm. (I) Quantification of average muscle fiber area from images depicted in Fig. 3H. AAV = adeno-associated virus; TA = tibialis anterior; Flag-GFP = FLAG-tagged green fluorescent protein; Flag-ChREBP-β = FLAG-tagged carbohydrate-response element binding protein-β; *ChREBP* = carbohydrate-response element binding protein; *Fasn* = fatty acid synthase; *Acaca* = acetyl-CoA carboxylase alpha; *Acly* = ATP citrate lyase; *Pparg* = peroxisome proliferator activated receptor gamma; *Cebpa* = CCAAT enhancer binding protein alpha; *Adipoq* = adiponectin; *Fabp4* = fatty acid binding protein 4; TG = triglyceride. GFP treatment = AAV-Flag-green fluorescent protein; ChREBP treatment = AAV-Flag-ChREBP-β. All the results are shown as the means ± SEM; *P < 0.05, **P < 0.01, ***P < 0.001.

Table 5
Effects of ChREBP overexpression on lipogenic genes expression in TA muscle of chickens.

Tissue	Gene	Treatment		SEM	*P*-value
		GFP	ChREBP		
TA	*ChREBP*	1.00	5.54*	4.538	0.017
	Thrsp	1.00	1.76*	0.756	0.026
	Acaca	1.00	2.49*	1.496	0.021
	Acss1	1.00	1.66***	0.668	<0.001
	Acc1	1.00	1.68*	0.684	0.033

SEM = the standard error of the mean; TA = tibialis anterior; *ChREBP* = carbohydrate-response element binding protein; *Thrsp* = thyroid hormone responsive; *Acaca* = acetyl-CoA carboxylase alpha; *Acss1* = acyl-CoA synthetase short chain family member 1; *Acc1* = acetyl-CoA-carboxylase 1.
GFP treatment = AAV-Flag-green fluorescent protein; ChREBP treatment = AAV-Flag-ChREBP-β.
Data represent the mean value of 6 to 7 replicates each treatment (n = 6 to 7).
Values with asterisk represent statistically significant differences (*P < 0.05, ***P < 0.001).

Table 6
Effect of ChREBP overexpression on IMF content in TA muscle of chickens.

Item	Treatment		SEM	*P*-value
	GFP	ChREBP		
TG, μmol/g protein	98.32	135.30**	36.960	0.001

ChREBP = carbohydrate-response element binding protein; IMF = intramuscular fat; TA = tibialis anterior; SEM = the standard error of the mean; TG = triglyceride.
GFP treatment = AAV-Flag-green fluorescent protein; ChREBP treatment = AAV-Flag-ChREBP-β.
Data represent the mean value of 7 replicates each treatment (n = 7).
Values with asterisk represent statistically significant differences (**P < 0.01).

addition, adipogenic marker genes in TA muscles were also significantly up-regulated in the fructose-supplemented group (P < 0.05). Consistent with the alterations in molecular signatures, a 40% increase in IMF content was detected in the TA muscles of the fructose-drinking mice compared to the controls (P < 0.001;

Table 7
Effects of fructose supplementation in drinking water on growth performance and IMF deposition in mice.

Item	Treatment		SEM	*P*-value
	Control	Fructose		
Drinking water[1], mL/d	4.78	8.98***	0.572	<0.001
Feed intake[1], g/d	3.16	1.49***	0.102	<0.001
Caloric intake[1], kcal/d	11.88	12.55	0.641	0.321
Body weight (0 d)[2], g	18.68	18.65	0.491	0.947
Body weight (21 d)[2], g	21.74	21.57	0.568	0.767
Body weight (42 d)[2], g	22.65	23.00	0.569	0.536
Body weight (63 d)[2], g	23.65	23.84	0.683	0.789
Body weight (84 d)[2], g	24.48	24.77	0.786	0.720
Liver[2], g	0.99	1.05*	0.030	0.034
eWAT[2], g	0.32	0.36	0.030	0.179
iWAT[2], g	0.19	0.20	0.016	0.383
BAT[2], g	0.04	0.05	0.002	0.093
GA[2], g	0.26	0.27	0.006	0.690
TA[2], g	0.09	0.09	0.004	0.824
TG[2], μmol/g protein	52.90	75.66***	4.136	<0.001

IMF = intramuscular fat; SEM = the standard error of the mean; eWAT = epididymal white adipose tissue; iWAT = inguinal white adipose tissue; BAT = brown adipose tissue; GA = gastrocnemius; TA = tibialis anterior; TG = triglyceride.
Control treatment = tap water; Fructose treatment = 20% fructose water.
Values with asterisk represent statistically significant differences (*$P < 0.05$, ***$P < 0.001$).
[1] Data represent the mean value of 6 to 7 replicates each treatment ($n = 6$ to 7).
[2] Data represent the mean value of 8 to 10 replicates each treatment ($n = 8$ to 10).

Table 8
Effects of fructose supplementation in drinking water on the expression of lipogenic and adipogenic genes in TA muscles of mice.

Tissue	Gene	Treatment		SEM	*P*-value
		Control	Fructose		
TA	Lipid synthesis				
	ChREBP	1.00	2.64**	0.366	0.001
	Fasn	1.00	2.35*	0.472	0.040
	Acaca	1.00	4.87**	0.884	0.001
	Acly	1.00	3.23**	0.706	0.009
	Adipogenesis				
	Pparg	1.00	2.34**	0.332	0.002
	Cebpa	1.00	2.97*	0.771	0.029
	Adipoq	1.00	2.10**	0.282	0.004
	Fabp4	1.00	19.58**	5.322	0.006

SEM = the standard error of the mean; TA = tibialis anterior; *ChREBP* = carbohydrate-response element binding protein; *Fasn* = fatty acid synthase; *Acaca* = acetyl-CoA carboxylase alpha; *Acly* = ATP citrate lyase; *Pparg* = peroxisome proliferator activated receptor gamma; *Cebpa* = CCAAT enhancer binding protein alpha; *Adipoq* = adiponectin; *Fabp4* = fatty acid binding protein 4.
Control treatment = tap water; Fructose treatment = 20% fructose water.
Data represent the mean value of 6 to 7 replicates each treatment ($n = 6$ to 7).
Values with asterisk represent statistically significant differences (*$P < 0.05$, **$P < 0.01$).

Table 7). Hence, these data indicate that chronic activation of ChREBP by fructose consumption can induce IMF deposition in mice.

3.6. Activation of ChREBP by fructose administration increases IMF content in chickens

Based on the above findings, next, studies were designed to investigate whether dietary supplementation of fructose can increase IMF in chickens. Therefore, the CYC were fed ad libitum with 10% fructose or not for 4 wk. The results are shown in Tables 9 and 10. Interestingly, different with the mice, the chickens in both groups had similar consumption of water and feeds. Additionally, fructose supplementation did not affect bodyweight growth, but slightly increased abdominal fat weight ($P = 0.008$), while leaving

Table 9
Effects of dietary fructose supplementation on growth performance and IMF deposition in broiler chickens.

Item	Treatment		SEM	*P*-value
	Control	Fructose		
Drinking water[1], mL/d	298.50	283.00	21.510	0.488
Feed intake[1], g/d	136.70	129.40	5.608	0.219
Body weight (0 d)[1], g	1425.00	1422.00	19.210	0.880
Body weight (7 d)[1], g	1675.00	1685.00	36.770	0.794
Body weight (14 d)[1], g	1889.00	1867.00	39.870	0.587
Body weight (21 d)[1], g	2076.00	2060.00	57.770	0.792
Body weight (28 d)[1], g	2201.00	2188.00	66.020	0.840
Liver[2], g	36.17	37.77	1.619	0.336
Spleen[2], g	7.09	6.14	1.016	0.362
Heart[2], g	11.19	11.06	0.484	0.798
Abdominal fat[2], g	40.58	56.90**	5.433	0.008
Thigh muscle[2], g	144.20	155.90	6.581	0.092
Breast muscle[2], g	196.90	203.10	9.173	0.507
Thigh muscle rate[2], %	10.29	11.05	0.393	0.070
Breast muscle rate[2], %	14.18	14.47	0.456	0.532
CF (thigh muscle)[2], %	7.083	9.358*	0.9737	0.035
CF (breast muscle)[2], %	3.456	4.661*	0.5453	0.044
TG (thigh muscle)[2], μmol/g protein	117.4	162.7*	45.24	0.025
TG (breast muscle)[2], μmol/g protein	68.3	100.1*	31.76	0.016

IMF = intramuscular fat; SEM = the standard error of the mean; CF= crude fat; TG= triglyceride.
Control treatment = basal diet; Fructose treatment = basal diet supplemented with 10% fructose (purity ≥ 99%).
Values with an asterisk represent statistically significant differences (*$P < 0.05$, **$P < 0.01$).
[1] Mean values are based on 6 birds per replicate and 5 replicates per treatment.
[2] Data represent the mean value of 8 to 10 replicates each treatment ($n = 8$ to 10).

Table 10
Effects of dietary fructose supplementation on the expression of lipogenic genes in chicken muscles.

Tissue	Gene	Treatment		SEM	*P*-value
		Control	Fructose		
Thigh muscle	*ChREBP*	1.00	1.71*	0.301	0.039
	Thrsp	1.00	1.62	0.354	0.104
	Acaca	1.00	1.62	0.284	0.051
	Acss1	1.00	1.47*	0.190	0.029
	Acc1	1.00	1.18	0.268	0.510
	Scd1	1.00	1.71*	0.240	0.011
Breast muscle	*ChREBP*	1.00	1.99*	0.336	0.013
	Thrsp	1.00	1.94*	0.359	0.022
	Acaca	1.00	1.30	0.268	0.289
	Acss1	1.00	1.87**	0.219	0.002
	Acc1	1.00	1.25	0.184	0.194
	Scd1	1.00	1.09	0.221	0.697

SEM = the standard error of the mean; *ChREBP* = carbohydrate-response element binding protein; *Thrsp* = thyroid hormone responsive; *Acaca* = acetyl-CoA carboxylase alpha; *Acss1* = acyl-CoA synthetase short chain family member 1; *Acc1* = acetyl-CoA-carboxylase 1; *Scd1* = stearoyl-coenzyme A desaturase 1.
Control treatment = basal diet; Fructose treatment = basal diet supplemented with 10% fructose (purity ≥ 99%).
Data represent the mean value of 6 to 8 replicates each treatment ($n = 6$ to 8).
Values with asterisk represent statistically significant differences (*$P < 0.05$, **$P < 0.01$).

the percentages of breast muscles and thigh muscles not affected. Histological analysis further showed that fructose administration did not alter the muscle fiber areas (Fig. S1A to C). Interestingly, consistent with the effects seen in mice, fructose addition up-regulated *ChREBP* and lipogenic genes expression in both thigh and breast muscles ($P < 0.05$). In agreement with the lipogenic gene expression, the contents of IMF or crude fat in thigh muscles and breast muscles were both significantly increased ($P < 0.05$). Consistently, the muscles of fructose-treated chickens accumulated more lipids than the controls as showed by Oil red O staining

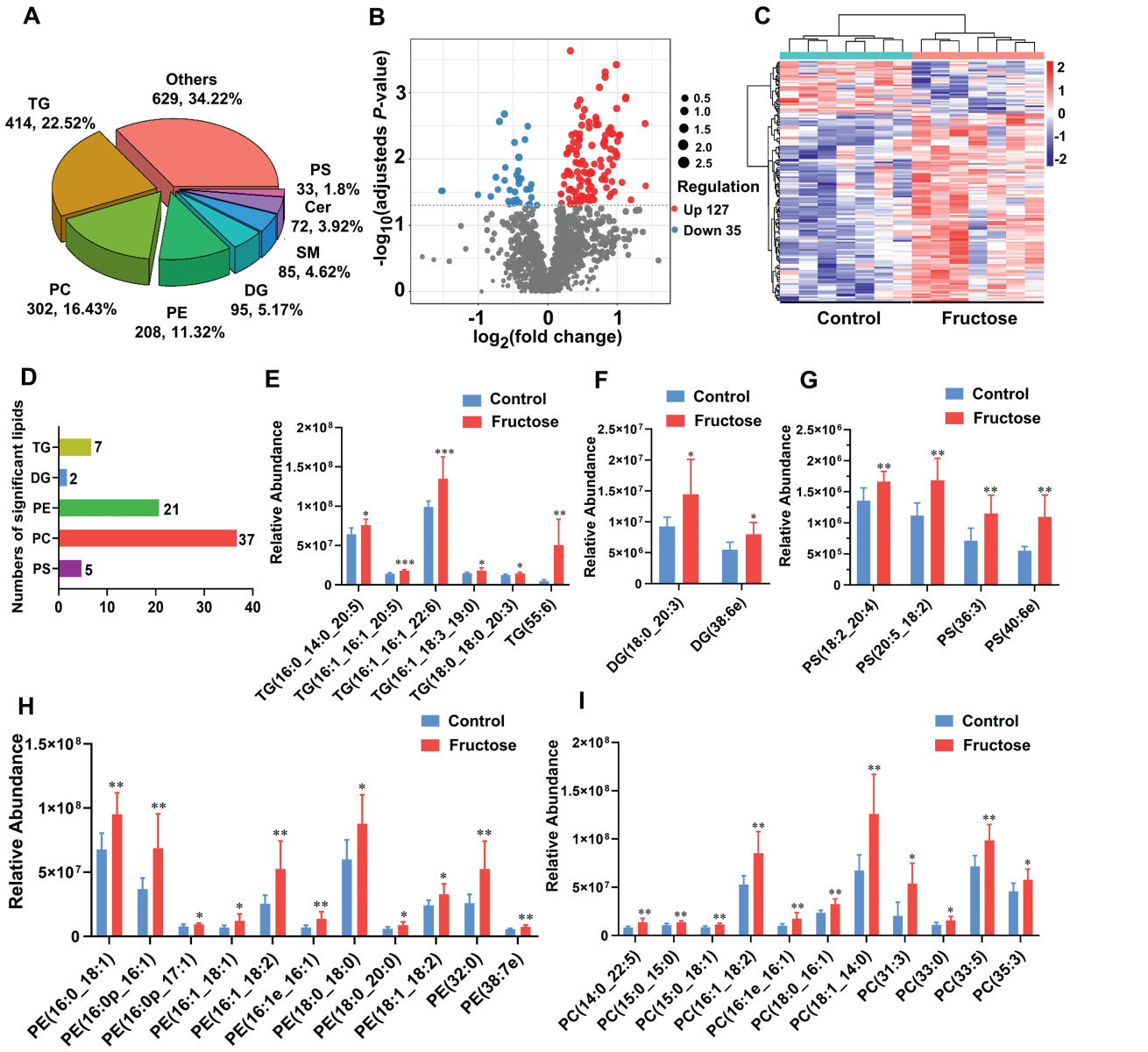

Fig. 4. Untargeted lipidomic analysis reveals dietary fructose supplementation remodels intramuscular fat (IMF) composition in chickens. (A) Percentages of lipid subclasses in TA muscles of control and fructose addition groups ($n = 7$). (B) Volcano plot comparison of lipid levels ($n = 7$). (C) Heat map analysis of all content-differential lipid molecules ($n = 7$). (D) The numbers of content-increased lipid molecules in fructose-fed group ($n = 7$). (E to I) The representative content-upregulated lipid molecules in each lipid subclass ($n = 7$). TG = triglyceride; DG = diglyceride; PS = phosphatidylserine; PE = phosphatidylethanolamine; PC = phosphatidylcholine; SM = sphingomyelin; Cer = ceramide. Control treatment = basal diet; Fructose treatment = basal diet supplemented with 10% fructose (purity ≥ 99%). All the results are shown as the means ± SEM; $^{*}P < 0.05$, $^{**}P < 0.01$, $^{***}P < 0.001$.

(Fig. S1D). Overall, these data suggest that fructose supplementation could activate ChREBP-mediated DNL pathway and increase IMF content in chickens.

3.7. Activation of ChREBP by fructose administration remodels meat lipid profiles in chickens

IMF content and composition are highly associated with meat flavor. Therefore, to investigate whether fructose administration in chickens can improve meat flavor, an untargeted lipidomic analysis was conducted to profile lipid alterations in TA muscles of the chickens. First, 1838 lipid species were identified in both groups, primarily belonging to classes such as TG (22.52%), phosphatidylcholine (PC, 16.43%), phosphatidylethanolamine (PE, 11.32%), diglyceride (DG, 5.17%), sphingomyelin (SM, 4.62%), ceramide (Cer, 3.92%) and phosphatidylserine (PS, 1.80%) (Fig. 4A). Then, 162 lipid species with differences in content were identified between the two groups (Fig. 4B). Of these, the content of 127 lipid species were increased, while the content of 35 lipid species were decreased (Fig. 4B). Cluster heatmap analyses of the differential lipid species revealed that the lipid species with increased content or decreased content belonged to distinct subclasses (Fig. 4C). Since fructose-induced DNL is believed to elevate lipid content, attention was paid on the species that showed a significant increase in lipid content, especially on the neutral lipids (TG and DG) and phospholipids (PE, PC, and PS) (Fig. 4D). The detailed information of these content-elevated lipid species is exhibited in Fig. 4E to I. To date, the functions of these lipid species are still largely unknown,

which could be investigated individually in the future study. Together, these data suggest that fructose administration in chickens remodels meat lipid composition, which may contribute to the improvement of meat flavor.

4. Discussion

IMF content is a key factor positively influencing meat quality (Khan et al., 2019). Nowadays, there is an urgent need to explore nutritional or genetic strategies to increase IMF content in animal production. ChREBP is an important transcription factor which can activate glycolytic and lipogenic genes expression in liver and adipose tissues in response to high carbohydrate environment (Iizuka and Horikawa, 2008; Uyeda and Repa, 2006). However, whether skeletal ChREBP plays a role in IMF deposition in farm animals is still unknown. In this study, skeletal ChREBP level was found to be positively correlated with IMF content in animals from chickens, pigs to mice. Skeletal overexpression of ChREBP promotes IMF deposition in vitro and in vivo. Moreover, activation of ChREBP by fructose administration elevates IMF content and remodels the lipid composition in chickens. Hence, this study found that activating ChREBP by fructose-rich diets provides a novel strategy to increase IMF deposition in farm animals.

In C2C12 myoblast, it was found that the retro-virus mediated overexpression of ChREBP-β dramatically elevated the total mRNA levels of *ChREBP* by hundreds of folds, however, at protein levels, it only increased about one fold, suggesting that a compensation event was occurred at the translational level, which can be verified in the future. While ChREBP-β was overexpressed at low levels, its overexpression remarkably promoted lipid accumulation in muscle cells under adipogenic conditions. This was a surprising finding because currently only a few genes were reported to have such strong pro-adipogenic effect in muscle cells (Seale et al., 2008; Zhu et al., 2015). Thus, ChREBP represents a new factor that induces myoblasts to deposit tremendous lipids. In terms of mechanism, as revealed by RNA-seq analysis, activation of lipid biosynthesis is the main reason for ChREBP-induced lipid accumulation in muscle cells. Interestingly, the pan-adipocyte marker genes, such as *Pparg*, CCAAT enhancer binding protein alpha (*Cebpa*), adiponectin (*Adipoq*), and fatty acid binding protein 4 (*Fabp4*), were also significantly up-regulated. This is probably due to the activation of PPARγ by the endogenous ligands produced through ChREBP-induced DNL (Witte et al., 2015). Meanwhile, despite lacking direct evidence, it is supposed that the inhibitory effect of C2C12 myogenesis by ChREBP overexpression is also linked to an increase in DNL (Hsueh et al., 2018; Jiang et al., 2022; Teboul et al., 1995).

Of note, skeletal overexpression of ChREBP-β in both mice and chickens by AAV injection also significantly facilitated IMF deposition. This is an important finding as the in vivo physiological environment is much more complicated than the in vitro environment. Since AAV is a relatively safe and increasingly used delivery tool for gene therapy (Daya and Berns, 2008; Dunbar et al., 2018; Mueller and Flotte, 2008), AAV expressing ChREBP-β may be used as a special reagent to improve the meat quality in animal production in the future.

Here, to provide a simple way to increase IMF content, a strategy was implemented involving dietary supplementation of fructose. That is because compared with other pro-lipogenic genes, one of the advantages of ChREBP is that it can be activated by metabolites of dietary glucose or fructose (Koo et al., 2009; Lanaspa et al., 2012). Dietary fructose has a more rapid and potent ability to activate ChREBP (Dushay et al., 2015; Kim et al., 2016), and fructose exerts pro-lipogenic effects independent of excess energy intake (Baena et al., 2016; Geidl-Flueck et al., 2021; Roncal-Jimenez et al., 2011), therefore we administered fructose water or supplement to the mice and chickens in this study. As expected, fructose addition elevated IMF deposition in both mice and chickens. In fact, it has been already known that in animal production high percentage of carbohydrate-rich diets have enabled the increase of IMF content and the improvement of the meat quality (Du et al., 2013; Graugnard et al., 2010; Mwangi et al., 2019). Thus, to some extent, our study provided a regulatory mechanism for how carbohydrate-rich diets promote IMF deposition in farm animals. Notably, based on the finding that activation of ChREBP inhibits myogenesis, it is suggested that fructose supplementation should be implemented in the late fattening stage of animal production to prevent any negative impact on meat yield.

Considering time and cost constraints, it is important to acknowledge that the study on fructose administration has certain limitations. Firstly, In addition to ChREBP, fructose can also activate MondoA, which is a paralog of ChREBP. MondoA positively regulates DNL and also contributes to IMF deposition (Ahn et al., 2019). Secondly, fructose can promote DNL not only in skeletal muscle cells but also in hepatocytes and adipocytes (Velázquez et al., 2022). As a result, on the one hand, lipids derived from the liver in the form of very low-density lipoproteins (VLDL) can contribute to the increase of IMF content by being taken up by muscles (Martínez-Uña et al., 2015); on the other hand, fructose-induced DNL in intramuscular adipocytes can also raise IMF content. Therefore, several different mechanisms can mediate fructose-stimulated IMF deposition, which warrants further investigation in the future.

5. Conclusion

This study investigated the role of ChREBP and fructose in lipid accumulation in muscle cells of mice and chickens. The findings suggest that skeletal ChREBP plays a crucial role in IMF deposition by inducing DNL. Activation of ChREBP by overexpression or fructose administration can both increase IMF deposition. This finding presents a potential strategy to improve meat quality in animal production through modulation of ChREBP activity. Moreover, these results have significant implications, shedding light on a regulatory mechanism through which diets rich in carbohydrates promote IMF deposition in farm animals.

Author contributions

Haihan Xiao and **Ziyi Song:** conceptualization. **Haihan Xiao** and **Tian Wu:** methodology. **Tian Wu:** software. **Qinghua Fu** and **Yameng Zhao:** validation. **Qinghua Fu** and **Peng Wang:** formal analysis. **Qinghua Fu:** investigation. **Haihan Xiao** and **Ziyi Song:** re-sources. **Peng Wang** and **Ziyi Song:** data curation. **Peng Wang** and **Haihan Xiao:** writing—original draft preparation. **Peng Wang**, **Haihan Xiao**, **Tian Wu**, **Xudong Song**, **Yameng Zhao**, **Yan Li**, **Jieping Huang**, and **Ziyi Song:** writing—review and editing. **Peng Wang**, **Haihan Xiao**, **Jieping Huang**, and **Ziyi Song:** visualization. **Ziyi Song:** supervision, project administration, funding acquisition. All authors have read and agreed to the published version of the manuscript.

Declaration of competing interest

We declare that we have no financial and personal relationships with other people or organizations that can inappropriately influence our work, and there is no professional or other personal interest of any nature or kind in any product, service and/or company that could be construed as influencing the content of this paper.

Acknowledgments

This research was funded by grants from the Specific Research Project of Guangxi for Research Bases and Talents (AD22035061), the National Natural Science Foundation of China (82100913 and 82360166), and the Project of Bama County for Talents in Science and Technology (20220016).

Appendix supplementary data

Supplementary data to this article can be found online at https://doi.org/10.1016/j.aninu.2024.04.006.

References

Ahn B, Wan S, Jaiswal N, Vega RB, Ayer DE, Titchenell PM, et al. MondoA drives muscle lipid accumulation and insulin resistance. JCI Insight 2019;4:e129119.
AOAC. Official methods of analysis. 19th ed. Gaithersburg, MD: AOAC International; 2012.
Baena M, Sangüesa G, Dávalos A, Latasa M-J, Sala-Vila A, Sánchez RM, et al. Fructose, but not glucose, impairs insulin signaling in the three major insulin-sensitive tissues. Sci Rep 2016;6:26149.
Bier A, Shapira E, Khasbab R, Sharabi Y, Grossman E, Leibowitz A. High-fructose diet increases renal ChREBPβ expression, leading to intrarenal fat accumulation in a rat model with metabolic syndrome. Biology 2022;11:618.
Chau GC, Im DU, Kang TM, Bae JM, Kim W, Pyo S, et al. mTOR controls ChREBP transcriptional activity and pancreatic β cell survival under diabetic stress. J Cell Biol 2017;216:2091–105.
Chen F-F, Xiong Y, Peng Y, Gao Y, Qin J, Chu G-Y, et al. miR-425-5p inhibits differentiation and proliferation in porcine intramuscular preadipocytes. IJMS 2017;18:2101.
Daya S, Berns KI. Gene therapy using adeno-associated virus vectors. Clin Microbiol Rev 2008;21:583–93.
Demirel G, Ozpinar H, Nazli B, Keser O. Fatty acids of lamb meat from two breeds fed different forage: concentrate ratio. Meat Sci 2006;72:229–35.
Du M, Huang Y, Das AK, Yang Q, Duarte MS, Dodson MV, et al. Meat science and muscle biology symposium: manipulating mesenchymal progenitor cell differentiation to optimize performance and carcass value of beef cattle1,2. J Anim Sci 2013;91:1419–27.
Dunbar CE, High KA, Joung JK, Kohn DB, Ozawa K, Sadelain M. Gene therapy comes of age. Science 2018;359:eaan4672.
Dushay JR, Toschi E, Mitten EK, Fisher FM, Herman MA, Maratos-Flier E. Fructose ingestion acutely stimulates circulating FGF21 levels in humans. Mol Metab 2015;4:51–7.
Filhoulaud G, Guilmeau S, Dentin R, Girard J, Postic C. Novel insights into ChREBP regulation and function. Trends Endocrin Met 2013;24:257–68.
Frank D, Joo S-T, Warner R. Consumer acceptability of intramuscular fat. Korean J Food Sci Anim 2016;36:699–708.
Fu Q, Liu X, Li Y, Wang P, Wu T, Xiao H, et al. Discovery of new inhibitors of eEF2K from traditional Chinese medicine based on in silico screening and in vitro experimental validation. Molecules 2022;27:4886.
Geidl-Flueck B, Hochuli M, Németh Á, Eberl A, Derron N, Köfeler HC, et al. Fructose- and sucrose- but not glucose-sweetened beverages promote hepatic de novo lipogenesis: a randomized controlled trial. J Hepatol 2021;75:46–54.
Graugnard DE, Berger LL, Faulkner DB, Loor JJ. High-starch diets induce precocious adipogenic gene network up-regulation in *longissimus lumborum* of early-weaned Angus cattle. Br J Nutr 2010;103:953–63.
Hausman GJ, Basu U, Du M, Fernyhough-Culver M, Dodson MV. Intermuscular and intramuscular adipose tissues: bad vs. good adipose tissues. Adipocyte 2014;3:242–55.
Hocquette JF, Gondret F, Baéza E, Médale F, Jurie C, Pethick DW. Intramuscular fat content in meat-producing animals: development, genetic and nutritional control, and identification of putative markers. Animal 2010;4:303–19.
Hsueh T-Y, Baum JI, Huang Y. Effect of eicosapentaenoic acid and docosahexaenoic acid on myogenesis and mitochondrial biosynthesis during murine skeletal muscle cell differentiation. Front Nutr 2018;5:15.
Iizuka K, Horikawa Y. ChREBP: a glucose-activated transcription factor involved in the development of metabolic syndrome. Endocr J 2008;55:617–24.
Iizuka K, Bruick RK, Liang G, Horton JD, Uyeda K. Deficiency of carbohydrate response element-binding protein (ChREBP) reduces lipogenesis as well as glycolysis. Proc Natl Acad Sci U S A 2004;101:7281–6.
Jiang A, Guo H, Zhang L, Jiang X, Zhang X, Wu W, et al. Free fatty acid impairs myogenic differentiation through the AMPK α-MicroRNA 206 pathway. Mol Cell Biol 2022;42:e00327-21.
Kato T, Iizuka K, Takao K, Horikawa Y, Kitamura T, Takeda J. ChREBP-knockout mice show sucrose intolerance and fructose malabsorption. Nutrients 2018;10:340.
Khan Raza, Junjvlieke Xiaoyu, Garcia Elnour, et al. Function and transcriptional regulation of bovine TORC2 gene in adipocytes: roles of C/EBP, XBP1, INSM1 and ZNF263. IJMS 2019;20:4338.
Kim M-S, Krawczyk SA, Doridot L, Fowler AJ, Wang JX, Trauger SA, et al. ChREBP regulates fructose-induced glucose production independently of insulin signaling. J Clin Investig 2016;126:4372–86.
Kirchgessner M, Roth F-X. Schätzgleichungen zur Ermittlung des energetischen Futterwertes von Mischfuttermitteln für Schweine. Z Tierphysiol Tierernähr Futterm 1983;50:270–5.
Koo H-Y, Miyashita M, Simon Cho BH, Nakamura MT. Replacing dietary glucose with fructose increases ChREBP activity and SREBP-1 protein in rat liver nucleus. Biochem Biophys Res Commun 2009;390:285–9.
Lanaspa MA, Sanchez-Lozada LG, Cicerchi C, Li N, Roncal-Jimenez CA, Ishimoto T, et al. Uric acid stimulates fructokinase and accelerates fructose metabolism in the development of fatty liver. PLoS One 2012;7:e47948.
Li J, Tang C, Zhao Q, Yang Y, Li F, Qin Y, et al. Integrated lipidomics and targeted metabolomics analyses reveal changes in flavor precursors in psoas major muscle of castrated lambs. Food Chem 2020;333:127451.
Martínez-Uña M, Varela-Rey M, Mestre D, Fernández-Ares L, Fresnedo O, Fernandez-Ramos D, et al. S-Adenosylmethionine increases circulating very-low density lipoprotein clearance in non-alcoholic fatty liver disease. J Hepatol 2015;62:673–81.
Meng J, Feng M, Dong W, Zhu Y, Li Y, Zhang P, et al. Identification of HNF-4α as a key transcription factor to promote ChREBP expression in response to glucose. Sci Rep 2016;6:23944.
Ministry of Agriculture of the People's Republic of China. China National feeding standard of chicken (NY/T 33-2004). Beijing, China: China Agriculture Press; 2004.
Mueller C, Flotte TR. Clinical gene therapy using recombinant adeno-associated virus vectors. Gene Ther 2008;15:858–63.
Mwangi FW, Charmley E, Gardiner CP, Malau-Aduli BS, Kinobe RT, Malau-Aduli AEO. Diet and genetics influence beef cattle performance and meat quality characteristics. Foods 2019;8:648.
Park M-J, Kim D-I, Lim S-K, Choi J-H, Han H-J, Yoon K-C, et al. High glucose-induced O-GlcNAcylated carbohydrate response element-binding protein (ChREBP) mediates mesangial cell lipogenesis and fibrosis. J Biol Chem 2014;289:13519–30.
Roncal-Jimenez CA, Lanaspa MA, Rivard CJ, Nakagawa T, Sanchez-Lozada LG, Jalal D, et al. Sucrose induces fatty liver and pancreatic inflammation in male breeder rats independent of excess energy intake. Metabolism 2011;60:1259–70.
Rosenvold K, Andersen HJ. Factors of significance for pork quality—a review. Meat Sci 2003;64:219–37.
Seale P, Bjork B, Yang W, Kajimura S, Chin S, Kuang S, et al. PRDM16 controls a brown fat/skeletal muscle switch. Nature 2008;454:961–7.
Song Z, Xiaoli AM, Zhang Q, Zhang Y, Yang EST, Wang S, et al. Cyclin C regulates adipogenesis by stimulating transcriptional activity of CCAAT/enhancer-binding protein α. J Biol Chem 2017;292:8918–32.
Song Z, Xiaoli AM, Li Y, Siqin G, Wu T, Strich R, et al. The conserved mediator subunit cyclin C (CCNC) is required for brown adipocyte development and lipid accumulation. Mol Metab 2022;64:101548.
Teboul L, Gaillard D, Staccini L, Inadera H, Amri E-Z, Grimaldi PA. Thiazolidinediones and fatty acids convert myogenic cells into adipose-like cells. J Biol Chem 1995;270:28183–7.
Uyeda K, Repa JJ. Carbohydrate response element binding protein, ChREBP, a transcription factor coupling hepatic glucose utilization and lipid synthesis. Cell Metab 2006;4:107–10.
Velázquez AM, Bentanachs R, Sala-Vila A, Lázaro I, Rodríguez-Morató J, Sánchez RM, et al. ChREBP-driven DNL and PNPLA3 expression induced by liquid fructose are essential in the production of fatty liver and hypertriglyceridemia in a high-fat diet-fed rat model. Mol Nutr Food Res 2022;66:2101115.
Wallace M, Metallo CM. Tracing insights into de novo lipogenesis in liver and adipose tissues. Semin Cell Dev Biol 2020;108:65–71.
Wang H, Wollheim CB. ChREBP rather than USF2 regulates glucose stimulation of endogenous L-pyruvate kinase expression in insulin-secreting cells. J Biol Chem 2002;277:32746–52.
Wang X, Yang J, Yao Y, Shi X, Yang G, Li X. AQP3 facilitates proliferation and adipogenic differentiation of porcine intramuscular adipocytes. Genes 2020;11:453.
Wang P, Wu T, Fu Q, Liao Q, Yan Li, Huang T, et al. Maternal high-fructose intake activates myogenic program in fetal brown fat and predisposes offspring to diet-induced metabolic dysfunctions in adulthood. Front Nutr 2022;9:848983.
Witte N, Muenzner M, Rietscher J, Knauer M, Heidenreich S, Nuotio-Antar AM, et al. The glucose sensor ChREBP links de novo lipogenesis to PPARγ activity and adipocyte differentiation. Endocrinology 2015;156:4008–19.
Yamashita H, Takenoshita M, Sakurai M, Bruick RK, Henzel WJ, Shillinglaw W, et al. A glucose-responsive transcription factor that regulates carbohydrate metabolism in the liver. Proc Natl Acad Sci U S A 2001;98:9116–21.
Zhu Y, Yang R, McLenithan J, Yu D, Wang H, Wang Y, et al. Direct conversion of human myoblasts into brown-like adipocytes by engineered super-active PPARγ: conversion of human myoblasts to brown-like adipocytes. Obesity 2015;23:1014–21.